Volume 12, Issue 3: July - September 2025



ADVANCEMENTS IN NUCLEATION THEORY: EXTENSIONS TO THE XPFC MODEL AND APPLICATIONS IN PRECIPITATION

Sahil Sekhri

Director
Golden dots international Pvt Ltd

Abstract—This paper explores significant advancements in nucleation theory by extending the binary X-point Free Energy Composition (XPFC) model to better capture the complexities of precipitation processes. Initially, two key extensions are introduced: the incorporation of an enthalpy of mixing to address non-ideal mixing behaviors and a general phenomenology for modeling density pair correlation functions. These enhancements enable a more accurate representation of equilibrium phase diagrams, including the ability to reproduce metastable features such as submerged liquid spinodals below eutectic points. The study applies these improvements to investigate multistep nucleation pathways in precipitation processes, particularly in the context of gold nanoparticles. The results demonstrate that the improved XPFC model effectively captures the kinetic pathways observed experimentally, revealing a rich landscape of nucleation behaviors. The findings highlight the impact of quench parameters, solution concentration, and particle polydispersity on nucleation kinetics. Future applications of the improved XPFC model include examining the effects of elasticity on nucleation in monotectic and syntectic systems, as well as addressing stability issues in nanocrystalline binary alloys. This research underscores the model's potential to provide deeper insights into various materials science phenomena beyond precipitation.

I. INTRODUCTION

The study of alloys in materials physics holds broad significance due to the strong dependence of material properties on microstructure, which evolves through non-equilibrium phase transformations during formation. This impacts diverse industries such as steel, aluminum, nano-fabrication, and opto-electronics. A key paradigm for understanding complex alloy microstructures is the binary alloy.

Binary alloys exhibit a rich diversity of properties due to their dependence on processing paths, microstructural features like grain boundaries and dislocations, and solidification processes. Constructing models to explain these behaviors is crucial. Current models of alloy solidification are categorized by length and time scales, ranging from continuum methods for macroscopic scales, Phase Field methods for mesoscopic scales, and Phase Field Crystal (PFC) methods for nanoscopic changes.

This thesis focuses on extending the binary XPFC model, a variant of PFC theory that enables simulation of a wide range of crystal symmetries. While binary PFC models have been successful in describing phenomena such as eutectic and dendritic solidification, clustering, and epitaxial growth, limitations remain in their description of phase diagrams and correlation functions. The XPFC model improves upon the original PFC by providing a more robust phenomenology for modeling correlation functions and crystal structures.

Despite these improvements, the binary XPFC model assumes a preferred structure at high and low concentrations, limiting its application in scenarios like syntectic phase diagrams, where intermediate concentration structures are significant. Additionally, the XPFC model assumes an ideal free energy of mixing, which restricts its ability to describe non-ideal alloy systems.

The research presented in this thesis aims to: (1) refine the XPFC theory with a more general phenomenology for pair correlation functions, (2) extend the free energy of mixing to account for non-ideality, and (3) use the new XPFC model to elucidate multi-step nucleation processes observed in diffusion-limited systems.

The remainder of this paper is structured as follows:

Chapter II introduces Classical Density Functional Theory (CDFT).

Chapter VI extends CDFT to solidification and introduces PFC theory.

Chapter X reviews binary PFC theory and existing alloy models.

Chapter XIV presents novel improvements to the XPFC binary alloy theory.

Chapter XVIII applies the new model to study multi-step nucleation of nanoparticles and discusses future applications.

II. INTRODUCTION TO CLASSICAL DENSITY FUNCTIONAL THEORY

Many physical theories are derived using a succession of approximations. While each approximation yields a theory that is more narrow, in scope, it is typically more tractable to either analytical or numerical analysis. Classical Density Functional Theory (CDFT) is derived using this approach and in this chapter we'll examine each approximation and the intermediate theory they supply.

CDFT is a theory of statistical mechanics. This means CDFT connects microscopic physics to macroscopic observables using statistical inference instead of attempting to compute microscopic equations of motion. The microscopic physics in this case is most accurately described by many-body quantum mechanics and so the theory of quantum statistical mechanics is a natural starting point in any attempt to calculate thermodynamic observables.

Statistical mechanics is not always described as statistical inference. See works of E. T. Jaynes for details on this approach [1]

We will see that for our systems of interest that the full quantum statistical theory is completely intractable. To preceed, we'll look at quantum statistical mechanics in the semi-classical limit. In the semi-classical limit we'll develop a theory of inhomogenous fluids called Classical Density Functional Theory (CDET). Finally, we'll see that constructing exact free energy functionals for CDFT is rarely possible and look at an approximation scheme for these functionals.

III. STATISTICAL MECHANICS IN THE SEMI-CLASSICAL

At a microscopic level, all systems are governed by the fundamental physics of quantum mechanics. Statistical mechanics and in particular quantum statistical mechanics provides a map between this microscopic reality and macroscopic thermodynamic observables. For most applications, quantum statistical mechanics is both intractable to analysis and contains more detail than necessary. For instance, the precise bosonic or fermionic nature of the particles in the system often has little consequence on the thermodynamic properties. We can ignore some of these quantum mechanical details by looking at statistical mechanics in the semi-classical limit.

For the sake of clarity, we'll look at a system of N identical particles in the canonical ensemble which is straightforward to generalize to multi-component systems and other ensembles. We start with the definition of the partition function for a system of many particles,

$$z = Ir_{\alpha\beta}^{h} i$$
, (1)

where,

 \hat{H} is the Hamiltonian $\frac{|\hat{\mathbf{q}}|^2}{2m} + V(\hat{\mathbf{q}})$, \mathbf{p} is set of particle momenta $(p_1, p_2, ..., p_N)$,

g is the inverse temperature $1/k_b T$ where k_b is the Boltzmann.constant.

Wigner [2], and shortly after, Kirkwood [3] showed that the partition function could be expanded in powers of h, facilitating the calculation of both a classical limit and quantum corrections to the partition function. Their method, the Wigner-Kirkwood expansion, involves evaluating the trace operation over a basis of plane wave solutions,

$$Z(\theta) = \frac{d\mathbf{q}d\mathbf{p}}{(200)^{N}} e^{-\frac{b-q}{2}} e^{-\theta H^{2}} e^{\frac{b-q}{2}} = \frac{d\Gamma(\mathbf{q}, \mathbf{p})}{d\Gamma(\mathbf{q}, \mathbf{p})}$$
 (2)

Where, $d\Gamma$ is the phase space measure $dpdq/(2\pi\hbar)^N$. To compute the integrand, ((q, p), we follow Uhlenbeck and Bethe [4] and first compute its derivative,

$$\frac{\partial l(\mathbf{q}, \mathbf{p})}{\partial a} = \mathbf{a} \underbrace{\overset{\text{max}}{\longrightarrow}}_{b} He^{-\frac{\mathbf{max}}{\longrightarrow}} I(\mathbf{q}, \mathbf{p}). \tag{3}$$

We then make a change of variables, $\ell(\mathbf{q}, \mathbf{p}) = e^{-\theta H} W(\mathbf{q}, \mathbf{p})$, where His the classical Hamiltonian. The new function $W(\mathbf{q}, \mathbf{p})$ encodes the deviation from classical behaviour due to a lack of commutation of the potential and kinetic energy terms in the Hamiltonian. Substituting this redefined form of

(q, p) into equation 3, using the explicit form of the quantum Hamiltonian and after a considerable amount of algebra we find a partial differential equation for W,

$$\frac{\partial W}{\partial O} = \frac{h^2}{2} \times_{\mathbf{q}} \times_{\mathbf$$

As in typical in perturbation theories, the solution can be expanded in a power series of a small number, in this case, h, according to $W = 1 + \hbar W_1 + \hbar^2 W_2 + By$ substituting this expansion into $I(\mathbf{q}, \mathbf{p}) = e^{-gH}W(\mathbf{q}, \mathbf{p})$ and $I(\mathbf{p}, \mathbf{q})$ back into equation 2 we find a power series expansion for the partition function as well,

$$Z = 1 + h \left(W^{\frac{1}{2}} \right) + h^{2} \left(W^{\frac{3}{2}} \right) + \dots \quad dCe^{\theta H}. \quad (5)$$

Where the average, (\cdot) , denotes the the classical average,

$$\langle A(p, q) \rangle = \frac{1}{Z} \int_{\mathbb{R}^{3}} dr A(p, q) e^{-\theta H}.$$
 (6)

Solving equation 4 to second order in h and computing the classical averages in equation 5 the quantum corrections to the classical partition are computed to second order as2,

$$\langle W_1 \rangle = 0,$$
 (7)
 $\langle W_2 \rangle = -\frac{\kappa^3}{24m} |\nabla_{\mathbf{q}} \underline{V}|^2$. (8)

The first order term is zero because $W_{\lambda}(\mathbf{q}, \mathbf{p})$ is an odd function of p. In terms of the Helmholtz free energy, for example, the corrections to second order would be,

F =
$$F_{classical} + \frac{\hbar^2 \beta^2 D}{74m} |\nabla_{\mathbf{q}} \nabla_{\mathbf{q}} \nabla_{\mathbf{q}$$

There are a few items of importance in equation 9. First of all, the correction is inversely proportional to both the temperature and the particle mass. For copper at room temperature, for instance, the prefactor $h^2 \theta^2 / (24m)$ is $O(10^{-4})$ or at its melting temperature the prefactor is O (10-6). The correction is also proportional to the mean of the squared force felt by each particle. So high density materials will have a higher quantum correction because they sample the shortrange repulsive region of the pair potential more than their low density counter parts.

A. Indistinguishability

There is an important distinction to be made between the quantum theory and the theory in the semi-classical limit. The integral over phase space of the partition function must only take into account the physically different states of the system. In the quantum theory this is achieved by tracing over any orthonormal basis of the Hilbert space, but in the classical theory we need to be careful not to double count states involving

²For detailed calculations see [5].

identical particle configurations. Classically, exchange of two identical particles does not result in a physically different state and thus these states should be considered only once in the sum over states in the partition function. More precisely, we should write the classical partition function as,

$$Z = \frac{\int_{-\theta}^{\theta} d\theta}{d\theta},$$
 (10)

Where the primed integral denotes integration only over the physically distinct states. In the common case of N identical particles, the phase space integral becomes,

$$dL \rightarrow \frac{1}{NL} \int dL$$
 (11)

Aggregating our results, we can thus write the partition function in the semi-classical limit as.

$$Z^{(6)} = \frac{1}{N!} \int_{N!} d\zeta e^{-\beta H} + Q(\bar{p}^2),$$
 (12)

Or, in the grand canonical ensemble,

$$\Xi(\mu, \theta) = \frac{\epsilon}{N!} \frac{\epsilon \beta M}{N!} \int_{\mathbb{R}^{2}} d\mathbb{L} e^{-\theta H} + O(\hbar^{2})$$
 (13)

Of course, to first order in h, this is exactly the form taught in introductory courses on statistical mechanics and derived by Gibbs3 prior to any knowledge of quantum mechanics [6]. The key insight here is to understand, in a controlled way, when this approximation is accurate and the magnitude of the next quantum correction is as seen in equation 9. We now apply this semi-classical limit of statistical mechanics to the study of the local density field.

IV. CLASSICAL DENSITY FUNCTIONAL THEORY

Ostensibly, when we study formation and evolution of microstructure in solids, our observable of interest is the density field. As per usual in theories of statistical thermodynamics we must distinguish between microscopic operators and macroscopic observables (the later being the ensemble average of the former). In classical statistical mechanics, operators are simply functions over the phase space, r. We use the term operator to make connection with the quantum mechanical theory. In the case of the density field, the microscopic operator is the sum of Dirac delta functions at the position of each particle,

$$\rho^{\circ}(x; \mathbf{q}) = \sum_{i=0}^{\underline{S}} \delta_{i}^{(3)} (x - q_{i})$$
 (14)

From which the thermodynamic observable is.

$$g(x) = \langle \rho^{*}(x; \mathbf{q}) \rangle = \text{Tr} \left[\rho^{*}(x; \mathbf{q}) f(\mathbf{q}, \mathbf{p}) \right]$$
 (15)

Where, Ir [.] now denotes the classical trace,

Tr
$$[A(\mathbf{q}, \mathbf{p})f(\mathbf{q}, \mathbf{p})] \equiv \int_{N=0}^{\infty} \frac{1}{NJ} d[A(\mathbf{q}, \mathbf{p})f(\mathbf{q}, \mathbf{p}), (16)]$$

³The ⁷h in Gibbs' formula was justified on dimensional grounds and was simply introduced as a scaling factor with units of action $(I \cdot s)$

And, $f(\mathbf{q}, \mathbf{p})$ is the equilibrium probability density function,

$$f(\mathbf{q}, \mathbf{p}) = \frac{e^{-\theta(H-\mu N)}}{\Xi(\mu, \theta)}$$
 (17)

where H is the classical Hamiltonian, μ the chemical potential of the system and $\Xi(\mu, \delta)$ is the grand partition function of the system.

To construct a theory of the density field we review the usual methodology for statistical thermodynamics. We will do so in the frame of entropy maximization in which the entropy is maximized subject to the macroscopically available information. Taking the existence of an average of the density field, particle number and energy as the macroscopically available information, we can maximize then Gibb's entropy functional.

$$S[f(\mathbf{q}, \mathbf{p})] = -k_b Tc [f(\mathbf{q}, \mathbf{p}) ln (f(\mathbf{q}, \mathbf{p}))],$$
 (18)

subject to the aforementioned constraints (fixed average density, particle number and total energy) to find a probability density function of the form,

$$f(\mathbf{q}, \mathbf{p}) \propto \exp -\theta \quad H - \mu N + \exp(x)\rho^*(x)$$
 . (19)

Where, θ , μ and $\phi(x)$ are the Lagrange multipliers associated with constraints of average energy, number of particles and density respectively. As you might imagine, the constraints of average particle number and density are not independent and satisfy,

$$N = \frac{\int}{dx g^{*}(x)}, \quad (20)$$

We can combine their Lagrange multipliers into one,

$$f(\mathbf{q}, \mathbf{p}) \propto \exp -\theta(H - \frac{dx\psi(x)\rho^{*}(x))}{2}$$
, (21)

Where, $\psi(x) = \mu - \phi(x)$, is the combined Lagrange multiplier named the intrinsic chemical potential. Recalling that chemical potential is the change in Helmholtz free energy made by virtue of adding particles to the system,

$$\frac{\partial F}{\partial N} = \mu$$
 (22)

the interpretation of the intrinsic chemical potential follows as the Helmholtz free energy change due to particles being added to a specific location. We'll see this in more detail briefly where we'll see an analogous equation for the intrinsic chemical potential.

The objective of statistical theories is to compute the statistics of some observable (random variable) of choice. Two special sets of statistics provide a complete description of the observable's probability distribution: the moments and cumulants4. The calculation of moments and cumulants can be aided by use of generating functions. In the case of statistical mechanics the generating functions of moments and cumulants have special physical significance. The generating function

⁴See [7] for discussion of moments, cumulants and their importance in

of moments is closely related to the partition function and the generating function of cumulants is closely related to the associated thermodynamic potential.

In the case where the observable is the local density field, this is made somewhat more technical by the fact that the density is a function instead of a scalar variable. As such the partition function is more precisely called the partition functional as it depends on a function as input. The thermodynamic potential will thus also be a functional. Specifically, the grand canonical partition functional is,

$$\Xi[\psi(x)] = \text{Tr exp.} -\theta H + \theta \quad \underline{dx}\psi(x)\rho^{*}(x)$$
 . (23)

As alluded to above, the partition functional is a type of moment generating functional in the sense that repeated (functional) differentiation with respect to the intrinsic chemical potential yields moments of the density field:

$$\frac{\theta^{-n}}{\Xi} \frac{\delta^{n\Xi}[\psi]}{\delta \psi(x_1) \dots \delta \psi(x_n)} = \langle \rho^*(x_1) \dots \rho^*_{\omega}(x_n) \rangle. \quad (24)$$

Similarly, we can construct a thermodynamic potential by taking the logarithm of the partition function. This potential in particular is called the grand potential functional in analogy with the grand potential of thermodynamics,

$$Q[\psi(x)] = -k_b T \log (\Xi[\psi(r)])$$
. (25)

The grand potential functional is a type of cumulant generating functional in the sense that repeated functional differentiation yields cumulants of the density field:

$$-\theta^{-n+1} \frac{\delta^n \Omega(\psi)}{\delta \psi(x_1) \dots \delta \psi(x_n)} - \langle \rho^n(x_1) \dots \rho^n_n(x_n) \rangle_c \quad (26)$$

Where, $\langle \cdot \rangle_{\infty}$ denotes the cumulant average [7].

If we examine the first two cumulants,

$$-\frac{\delta \Omega I \psi l}{\delta \psi f(x)} = \langle \rho^{\wedge}(x) \rangle \equiv \rho(x), \qquad (27)$$

$$-k_{h}T \frac{\sigma^{-}(x) \psi l}{\delta \psi (x) \delta \psi(x)} = \langle (\rho^{\wedge}(x) - \rho(x)) \langle \rho^{\wedge}(x) - \rho(x) \rangle \rangle, \qquad (28)$$

we notice two remarkable things: The first, implies that the average density field is a function of only its conjugate field, the intrinsic chemical potential, and the second implies that that relationship is invertible⁵. To see this, we compute the Jacobian by combining equation 27 and 28,

$$\frac{\delta \varrho(x)}{\delta \psi(x')} = \theta \left((\rho^*(x) - \rho(x))(\rho^*(x') - \rho(x')) \right). \quad (29)$$

The right hand side of equation 29 is an autocorrelation function and therefore positive semi-definite by the Weiner-Khinchin theorem [8]. This implies that, at least locally, the intrinsic chemical potential can always be written as a functional of the average density, $\psi[p(x)]$, and vice versa. Furthermore, because all of the higher order cumulants of the density depend on the intrinsic chemical potential, they too depend only on the average density.

Given the importance of the average density, $\rho(x)$, it follows that we would like to use a thermodynamic potential with a natural dependence on the density. We can construct a generalization of the Helmholtz free energy that has precisely this characteristic by Legendre transforming the Grand potential,

$$\mathbb{E}[\rho(x)] = \Omega[\psi[\rho]] + d\omega(x)\psi(x). \quad (30)$$

F[g(x)] is called the intrinsic free energy functional.

It can be shown [9] that $\rho(x)$ must be the global minimum of the grand potential, which sets the stage for the methodology of classical density functional theory: if we have a defined intrinsic free energy functional, F, we can find the equilibrium density field by solving the associated Euler-Lagrange equation,

$$\frac{\delta \Omega[\rho]}{\delta a(r)} = 0.$$
 (31)

Finally, we may construct an analogous equation to equation 22 for the intrinsic chemical potential,

$$\frac{\delta F}{\delta o(x)} = \psi(x),$$
 (32)

which follows from equation 30 assuming equation 31. Equation 32 implies that the intrinsic chemical potential is the free energy cost of adding density to the location x specifically.

V. Techniques in Density Functional Theory

The difficulty in formulating a density functional theory is, the construction of an appropriate free energy functional. While exact calculations are rarely feasible, there are a variety of techniques that help in building approximate functionals. It is important to note first what we can compute exactly. In the case of the ideal gas, we can compute the grand potential and ree energy functional exactly.

$$\Omega_{id}[\psi] = -\frac{k_b T}{\Lambda_3} \int_{\partial X} dX e^{\theta \psi(x)}$$
(33)

$$F_{id}[\rho] = k_b I$$
 dx $\rho(x) |_{\Omega} \wedge^3 \rho(x) - \rho(x)|_{\infty}$ (34)

Where A is the thermal de Broglie wavelength,

$$\Lambda = \frac{2\pi h^2}{mk_bT}$$
(35)

We may then express deviation from ideality by factoring the ideal contribution out of the partition function,

$$\Xi[\psi] = \Xi_{int}[\psi]\Xi_{int}[\psi],$$
 (36)

leading to grand potential and free energy functionals split into ideal and excess components,

$$\Omega = \Omega_{id} + \Omega_{ex}$$
 (37)

$$F = F_{id} + F_{our} \qquad (38)$$

⁵The inverse function theorem only implies local invertibility, there is no guarentee of global invertibility. Indeed phase coexistance is a manifestation of this fact where a single intrinsic chemical potential is shared by two phases

Volume 12, Issue 3: July - September 2025

The interaction potential, $V(\mathbf{q})$, in the excess partition function typically makes a direct approach to calculating the excess free energy intractable. Though perturbative methods, including the cluster expansion technique [10], have been developed to treat the interaction potential systematically, other approximation schemes for the excess free energy are typically more pragmatic, particularly where deriving models that are tractable for the numerical simulation of dynamics is concerned. In particular, we can approximate the excess free energy by expanding around a reference homogeneous fluid with chemical potential μ_0 and density ρ_0 ,

$$F_{ex}[\rho] = F_{ex}[\rho_0] + \frac{\delta F_{ex}}{\delta \rho(x)} \underset{\rho_0}{\sim} * \Delta \rho(x)$$

$$+ \frac{1}{2} \Delta \rho(x') * \frac{\delta^2 F_{ex}}{\delta \rho(x) \delta \rho(x')} \underset{\rho_0}{\sim} * \Delta \rho(x)$$

$$+ \dots \qquad (39)$$

where $\Delta \rho(x) = \rho(x) - \rho_0$ and we have introduced the notation, * to mean integration over repeated co-ordinates, for example,

$$f(x') * g(x') \equiv dx'f(x')g(x').$$
 (40)

The excess free energy is the generating functional of a family of correlation functions called *direct correlation functions*,

$$\frac{\delta^{\alpha} \mathbb{E}_{\omega}[\rho]}{\delta \varrho(x_1) \dots \delta \varrho(x_{\omega})} = -\beta C \, \varrho(x_1, \dots, x_{\omega}), \quad (41)$$

the first of which, for a uniform fluid, is the excess contribution to the chemical potential. We may express this as the total chemical potential less the ideal contribution (see equation 34),

$$\frac{\delta E_{uv}}{\delta \rho} = \mu_0^{ex} = \mu_0 - \mu_{ud} = \mu_0 - k_d T \ln \lambda^3 R^{0}$$
 (42)

Truncating the expansion in equation 39 to second order in $\Delta \rho(x)$ and substituting the linear and quadratic terms from equation 42 and 41, we can simplify the excess free energy to

$$E_{\nu}[\rho(r)] = E_{\nu}[\rho_0] + \frac{dr}{dr} \mu - \frac{k_B T}{L_{\rm in}} \Lambda^8 \rho_0 \quad \Delta \rho(r) \\ - \frac{k_B T}{2} \Delta \rho(r) + C_0 \quad (r, r') + \Delta \rho(r'),$$
(43)

where $C_0^{(2)}(r, r')$ denotes the two-point direct correlation function at the reference state. Combining equation 34 with the simplified excess free energy in equation 43, we can express total change in free energy, $\Delta F = F - F[\rho_0]$, as,

total change in free energy,
$$\Delta F = \Gamma - \xi[\rho_0]$$
, as,

$$\Delta E[\rho(r)] = k T \quad dr \quad \rho(r) \ln \frac{\rho(r)}{r} - (1 - \beta \mu) \Delta \rho(r)$$

$$- \frac{k \pi T}{2} \Delta \rho(r) * C_0^{(2)}(r, r') * \Delta \rho(r').$$
(44)

We find an equivalent expression for the grand potential

after a Legendre transform,

$$\Delta\Omega[\rho(r)] = k_B T \operatorname{d} r \quad \varrho(r) \ln \frac{\varrho(r)}{\rho_0} + \varrho \varphi(r) - \Delta \rho(r) - \frac{\Delta g_{L}}{2} + \frac{2}{2} \operatorname{d} \rho(r) + C_0^{(2)}(r, r') + \Delta \rho(r').$$
(45)

where $\phi(r)$ is defined as an external potential, introduced into the system for completeness.

We see that the density functional theory derived here can be derived through a series of approximations from a fundamental basis in quantum statistical mechanics and requires no more parameters, than the thermodynamic details of a homogeneous reference fluid. It is reasonable to ask at this point whether or not we have really gained anything with this approximation scheme. Although we have arrived at a relatively simple form for the free energy functional, we've added several parameters to the functional based on the reference fluid. Thankfully, the theory of homogeneous liquids is very well established. This implies we may rely on a broad choice of analytical, numerical or experimental techniques to derive these parameters.

Equation 44 establishes an approximate density functional theory for inhomogenous fluids. However, as we will see in the following chapter, the properties of the direct correlation function $C_0^2(r, r')$ also carries information about how the fluid solidifies in the solid state as temperature or density cross into the coexistence.

The classical density functional theories derived in chapter II were first established to study inhomogenous fluids. By considering the solid state as an especially extreme case of an inhomogeneous fluid [11], we can use CDFT to study the process of solidification. From the perspective of CDFT, solidification occurs once the density field develops long range periodic structure. While not expressed in precisely this language, this approach dates back as far as 1941 with the early work of Kirkwood and Monroe [12] and was later significantly refined by Yussouff and Ramakrishnan [13].

We'll see that the approach of Youssof and Ramakrishnan was very successful at explaining the solidification in the thermodynamic sense. That is to say, it elucidates the parameters responsible for solidification but not the dynamical pathway responsible for the transition. To discuss the pathway toward equilibrium and the non-equilibrium artifacts introduced along the way into many solids (e.g. grain boundaries, vacancies, dislocations, etc.) we proceed to extend the CDFT framework using the Dynamic Density Functional Theory (DDFT). Noting that the full DDFT framework can be intractable in practice, we conclude by introducing a simplified density functional theory called the Phase Field Crystal (PFC) theory.

VII. AMPLITUDE EXPANSIONS

To explore the problem of solidification, we begin with the approximate grand potential established in equation 45 with the external potential, $\phi(r)$, set to zero,

$$\beta\Delta\Omega[\rho(r)] = dr \rho(r) \ln \frac{\rho(r)}{\rho_0} - \Delta\rho(r)$$

$$= \frac{1}{2}\Delta\rho(r) + C_0^{(2)}(r, r') + \Delta\rho(r'). \quad (46)$$

To make our theory concrete we must choose a suitable reference liquid to set the parameters ρ_0 and $C_0^{(2)}(r, r')$. We will choose the reference liquid to be the liquid at the melting point with density ρ_0 .

Scaling out a factor of ρ_{c} we can rewrite the grand potential in terms of a dimensionless reduced density, $n(r) = (\rho(r) - \rho_{c})/\rho_{c}$

$$\frac{\beta \Delta Q[n(r)]}{\rho_{r}} = \frac{\int_{-\infty}^{\infty} dr \{(1 + n(r)) \ln_{r}(1 + n(r)) - n(r)\}}{-\frac{1}{2} n(r) + \rho_{r}Q^{(2)}(r, r') + n(r')}. (47)$$

To approximate the density profile in the solid state we can expand the density in a plane waves,

$$\rho(r) = \bar{n} + \sum_{\mathbf{G} \in \mathcal{G}_{r}} \xi_{\mathbf{G}} \xi_{\mathbf{G}_{r}}^{\mathbf{G}_{r}}$$
(48)

Where G is the set of reciprocal lattice vectors in the crystal lattice and the amplitudes, ξ_{G} serve as order parameters for freezing. \bar{h} is the k=0, or equivalently the spatial average, of the density profile. In the liquid phase all amplitudes are zero and the average density is uniform, while in the solid phase there are finite amplitudes that describe the periodic profile of the crystal lattice. As we have chosen the reference fluid to be the liquid at the melting point with uniform density g_{in} \bar{h} is zero for the liquid phase at the melting point (for that reference density) and \bar{h} is the fractional density change of solidification, defined here as η , for the solid phase at the melting point, where

$$\eta = \frac{\rho_s - \rho_l}{\rho_l}$$
(49)

and in which ρ_s is the macroscopic density of the solid phase. The amplitudes are constrained by the point group symmetries of the lattice. Grouping the amplitudes of symmetry-equivalent reciprocal lattice vectors together we can write the density profile as,

$$\underline{n}(r) = \bar{n} + \frac{\sum_{\alpha} \sum_{\alpha} \sum_{\beta \in \mathbf{S}_{\alpha}} | \Box}{\xi_{\alpha} + \xi_{\alpha} + \xi_{\alpha}}, \quad (50)$$

Where α is a label running over sets of symmetry-equivalent reciprocal lattice vectors. More precisely, if we apply the projection operator of the totally symmetric representation of the lattice point group to the reciprocal lattice vectors we may label the distinct linear combinations ⁶ with α [14]. The members of these distinct linear combinations form the set $\{G\}_{\alpha}$. If we insert equation 50 into equation 47 and integrate over the unit cell of the particular crystal we wish to develop the theory for, we find,

$$\frac{\partial \Delta \Omega_{cell}}{\partial r} = \int_{0}^{\infty} d\zeta \left\{ (n(r) + 1) \ln (n(r) + 1) - n(r) \right\} \\ - \frac{1}{\tilde{n}^2} \rho \tilde{\zeta}_{n}^{(2)}(0) + \frac{2}{\tilde{n}^2} \rho \tilde{\zeta}_{n}^{(2)}(\mathbf{G}_{n}) \lambda |\xi|^2_{\infty} \\ - \frac{1}{\tilde{n}^2} \ln 2 + \frac{2}{\tilde{n}^2} \ln$$

Where λ_{α} is the number of reciprocal lattice vectors in the set α and $\tilde{C}_0^{2}(k)$ is the Fourier transform of the direct correlation function of the reference fluid. The first term in equation 51 is convex in all of the amplitudes with a minimum at zero. It is noteworthy, as we will discuss shortly, that the product $\rho_*C_0^*(G_{\alpha})$ is a simple function of the structure factor, $S(k)^*$, namely,

$$p_{\ell}\tilde{C}_{0}^{2}(k) = \frac{S(k)-1}{S(k)} \quad \forall \ k/=0.$$
 (52)

It follows that solidification must occur when the product $\varrho_L \tilde{\zeta}_{\gamma_0}^{(2)}(\mathbf{G}_{\alpha})$ (or equivalently, the reference structure factor $S_0(\mathbf{G}_{\alpha})$) is large enough to stabilize a finite amplitude by creating a new minimum away from zero. This phenomenon is shown schematically in figure 1 where the grand potential is projected on to a particular ξ_{α} axis and plotted for different values of the reference structure factor. When the reference structure factors are less than some set of critical structure factors (denoted as $S_{\alpha}^{*}(\mathbf{G}_{\alpha})$), only zero amplitude solutions are stable. When the reference structure factors are critical both the zero and non-zero amplitude solutions are stable and we find liquid-solid coexistence. Once the reference structure factors are greater than critical one the periodic crystalline solutions is stable.

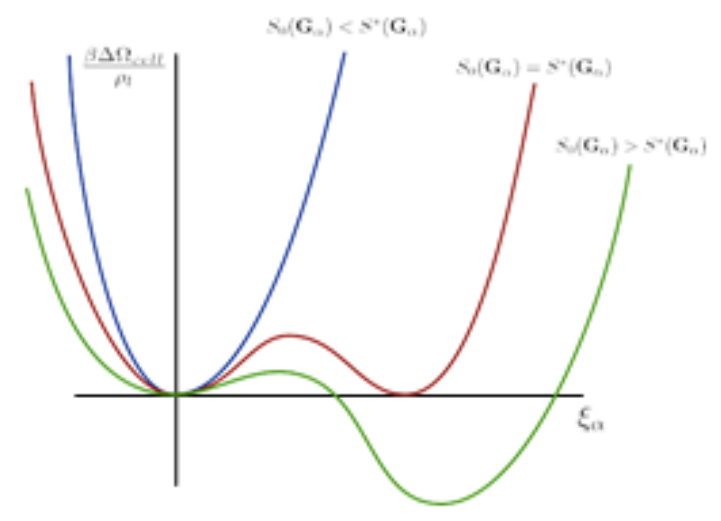


Fig. 1: Schematic view of the grand potential $\theta\Delta\Omega/\varrho_{\phi}$ projected on to an ξ_{α} axis for three different reference structure tactors. To minimize the grand potential, finite ξ_{α} is stable once $S_0(\mathbf{G}_{\alpha}) > S^*(\mathbf{G}_{\alpha})$

⁶These linear combinations are all formally equal to zero. It is important to treat opposite vectors (v and -v) as distinct for the sake of calculating the set $\{G_{ab}^{\dagger}\}$

⁷This follows from the definition of the structure factor and the Omstein-Zernike equation

Furthermore, equation 51 suggests that the set of critical structure factors, $\{S_n^*(\mathbf{G}_\alpha)_n\}$ are material independent as no free parameters remain in the grand potential. As a consequence, once we specify the symmetry of the lattice a liquid will solidify into (eg. face-centred-cubic), all materials that undergo this transition should share these parameters at the melting point.

Early numerical evidence of this result was supplied by the Hansen-Verlet criterion [15] which states that for a Lennard-Jones fluid the peak of the structure factor is constant along the melting curve with a <u>value at 2.85</u>. It has been noted that in comparing experimental evidence of a variety of liquids solidifying to fcc structure, most have a peak value close to 2.8 whereas those solidifying into bcc structures have a peak value around 3.0 [13].

At this level, the CDFT theory of solidification is an infinite order parameter theory of solidification. We can simplify the theory by truncating the number of amplitudes we keep in our expansion of the density. This is justified by noting that only terms from the first few reciprocal lattice families contain the majority of the grand potential energy of solidification[13].

As seen in table Ia and table Ib theoretical results from a single amplitude theory (theory I in the results) are poor but improve significantly with two order parameters (theory II) or higher order expansions of the free energy (theory III).

VIII. DYNAMIC DENSITY FUNCTIONAL THEORY

In spite of its successes, the CDFT theory of solidification cannot be a general description of solidification as many materials never fully reach equilibrium. The resulting microstructure affects the mechanical properties of the solid. In order to improve our theory we need to examine the pathway systems take to equilibrium so we can understand these microstructural features. We begin with a brief overview of non-equilibrium statistical mechanics.

A. Overview of Non-equilibrium Statistical Mechanics

Consider a non-equilibrium probability distribution over phase space, $f(\mathbf{q}, \mathbf{p}; t)$. As a function over phase space, its equation of motion is a simple result of classical mechanics,

$$\frac{df}{dt} = \{f, H\} + \frac{\partial f}{\partial t}$$
 (53)

Where $\{\cdot,\cdot\}$ denotes the Poisson bracket,

$$\{f, a\} = \frac{2^{N}}{\int_{i=0}^{\infty} \frac{\partial f}{\partial q_{i}} \frac{\partial g}{\partial p_{i}} - \frac{\partial g}{\partial q_{i}} \frac{\partial f}{\partial q_{i}} \frac{\partial g}{\partial p_{i}}}{\partial q_{i} \partial p_{i}} (54)$$

Of course, the distribution must remain normalized in time and therefore the total time derivative must be zero,

$$\int d\mathbf{q} d\mathbf{p} f(\mathbf{q}, \mathbf{p}; t) = 1 \xrightarrow{\underline{at}} = 0.$$
 (55)

Accounting for this conservation law in equation 53, the resulting equation of motion is called the Liouville Equation,

$$\frac{\partial f}{\partial t} = -\{f, H\}$$
 (56)

Under appropriate conditions the probability distribution, under the action of the Liqueille Equation, will decay to a stable fixed point $f_{ee}(\mathbf{q}, \mathbf{p})$ we call equilibrium,

$$\lim_{t\to\infty} f(\mathbf{q}, \mathbf{p}; t) - f_{oo}(\mathbf{q}, \mathbf{p}) \qquad (57)$$

Using the non-equilibrium probability distribution, we can also discuss non-equilibrium averages of the density profile and their associated equations of motion. The non-equilibrium density is written in analogy with equation 15 by taking of the classical trace of the density operator over with the nonequilibrium distribution,

$$g(\mathbf{x}, t) = \langle \rho^*(\mathbf{x}; \mathbf{q}) \rangle_{oe} = \operatorname{Tr} \left[\rho^*(\mathbf{x}; \mathbf{q}) f(\mathbf{q}, \mathbf{p}, t) \right].$$
 (58)

Where $(\cdot)_{ne}$ denotes the non-equilibrium average, (i.e., using $f(\mathbf{q}, \mathbf{p}, t)$). Just as the non-equilibrium probability distribution is, driven to equilibrium by the Liouville Equation, so too is the density profile by its own equation of motion.

B. Equation of Motion for the Density

A variety of equations of motion for the density field are known. For instance, we can consider the Navier-Stokes equations of hydrodynamics as one such equation of motion. If we restrict ourselves to diffusion limited circumstances, we may derive a much simpler equation of motion. To achieve this result we use the projection operator method, and assume that the density operator is the only relevant variable. Quoting the result from [8] we find,

$$\frac{\partial \rho(r, t)}{\partial t} = \nabla \cdot \underbrace{dr'}_{} \mathbf{D}(r, r', t) \cdot \nabla' \underbrace{\delta E[\rho]}_{} \rho (59)$$

where ∇' denotes differentiation with r', and $\mathbf{D}(r, r', t)$ is the diffusion tensor,

$$\mathbf{D}(r, r', t) = \int_{0}^{\infty} d\mathbf{r}' \mathbf{J} \mathbf{r}'' f(\mathbf{q}, \mathbf{p}, t) \hat{\mathbf{J}}(r, 0) \hat{\mathbf{J}}(r', \tau') \dots (60)$$

in which $\hat{J}(r, t)$ is the local density flux,

$$\hat{\mathbf{J}}(r, t) \equiv \underbrace{\frac{\mathbf{p}_i}{\partial \hat{\mathbf{p}}_i}}_{\mathbf{p}_i} \delta(r - q_i).$$
 (61)

Theories using equation 59 and variations thereof are often called *Dynamic Density Functional Theories* (DDFT) or at times *Time Dependent Density Functional Theories* (TDDFT) though we will use the former throughout this work.

The non-equilibrium diffusion tensor presents a significant impediment to integrating this equation of motion so in practice it is often approximated. Following [8], if we assume that the positions evolve more slowly than the velocities and that the momenta of different particles are uncorrelated we can dramatically, simplify the diffusion tensor,

$$D(r, r') = D_0 1 \rho(r, t) \delta(r - r').$$
 (62)

Where D_0 is the diffusion coefficient,

$$D_0 = \frac{1}{3m^2} \int_0^{\infty} dt \text{Tr} \left[f(\mathbf{q}, \mathbf{p}, t) p_i(0) \cdot p_i(t) \right]. \quad (63)$$

Theory	$\tilde{C}(\mathbf{G}_{[111]})$	č (G [811])	η
I	0.95	0.0	0.074
П	0.65	0.23	0.270
Ш	0.65	0.23	0.166
Experiment	0.65	0.23	0.148

 ⁽a) Freezing parameters for fcc, with comparison to Argon experimental results.

Theory	$\tilde{C}(\mathbf{G}_{[110]})$	č (G _[211])	η
I	0.69	0.00	0.048
П	0.63	0.07	0.052
Ш	0.67	0.13	0.029
Experiment	0.65	0.23	0.148

(b) Freezing parameters for bcc with comparison to Sodium experimental results.

TABLE I: Freezing parameters for fcc and bcc systems and comparison to experiment from [13]. Theory I uses one order parameter, theory II uses two order parameters and theory III uses two order parameters with a higher (third) order expansion in the free energy. A is the fractional density change of solidification from equation 49

Substituting into equation 59 we find a simplified equation of motion originally suggested by [16],

$$\frac{\partial o(r, t)}{\partial t} = \nabla \cdot D_0 \rho(r, t) \nabla \frac{\delta F[\rho]}{\delta \partial r, t}$$
 (64)

The equation of motion can also be written as a Langevin equation. In this variant the equation of motion is for the density, operator, ρ , and the noise is assumed to obey a generalized Einstein relation,

$$\frac{\partial \phi'(x-t)}{\partial t} = \nabla \cdot D_0 \phi^*(x-t) \nabla \cdot \frac{\partial F[\phi]}{\delta \phi^*} + \xi(x,t), \quad (65)$$

$$\langle \xi(x,t) \rangle = 0, \quad (66)$$

$$\langle \xi(x,t) \xi(x,t) \rangle = -2 \nabla \cdot [D_0 \phi(x,t) \nabla \delta(x-x) \delta(t-t)]. \quad (67)$$

See Appendix A for more details on generalized Einstein relations and [17] for a detailed discussion about equations 64 and 65.

At times, the diffusion tensor is assumed to be constant. This is common place in many Phase Field Crystal theories. In light of equation 64, this is akin to assuming the density yariations are small.

Unfortunately, if we were to use the approximate free energy functional established in equation 44 in the DDFT of equation 64 or 65 we would face a major impediment: the solid state solutions of the density functional theory approach yield sharply peaked solutions at the position of the atoms in the lattice. While this is realistic, they are a major challenge for numerical algorithms that aim to explore long-time microstructure evolution. The challenges are two-fold. First, these sharp peaks require a fine mesh to be resolved resulting in intractably large memory requirement to simulate domains of any non-trivial scale. Second, linear stability analysis of most algorithms demonstrates that the time step size is a monotonically increasing function of the grid spacing, thus only small time steps can be taken on a fine mesh. This further restricts the time scales of microstructure evolution that can be practicality explored to times scales comparable to those of molecular dynamics -perhaps somewhat longer.

One pragmatic solution to this problem is to further approximate the free energy functional of equation 44 in such a way as to produce a theory that retains the essential physics of solidification but produces a solid state that is more smoothly peaked. As we will see next, the Phase Field Crystal (PFC) theory, the topic of this thesis, aims to achieve precisely this balance.

IX. PHASE FIELD CRYSTAL THEORY

The phase field crystal theory (PFC) presents a solution to the aforementioned numerical difficulties faced by DDFT methods by approximating the free energy in such a way as to retain the basic features of the theory using a smoother solid state description of density. Starting with the approximate free energy functional of equation 44 we proceed as previously by scaling out a factor of the reference density and changing variables, to a dimensionless density $n(r) = (\rho(r) - \rho_s)/\rho_s$

$$\frac{\beta F[n(r)]}{\rho_r} = \int_{-\frac{\pi}{2}}^{\frac{\pi}{2}} dr \{ (n(r) + 1) \ln(n(r) + 1) - (1 - \beta \mu_0) n(r) \} - \frac{1}{2} n(r) + \rho \mathcal{E}_0^{(2)}(r, r) + n(r).$$
 (68)

We then Taylor expand the logarithm about the reference density or equivalently n(r) = 0, to fourth order,

$$\frac{\beta F[n(r)]}{\rho_{i}} = \int_{0}^{\infty} dr \frac{a(r)^{2}}{7} - \frac{a(r)^{6}}{6} + \frac{a(r)^{4}}{12} - \frac{1}{2}n(r) + \rho_{i}C_{0}^{(2)}(r, r) + n(r). \quad (69)$$

Where the linear term can be dropped by redefining the density o(r) shout its average. Most phase field crystal theories also use a simplified equation of motion as well,

$$\frac{\partial n(r, t)}{\partial t} = M \nabla^{2} \frac{\partial g_{\Gamma} [n(r)]}{\partial a(r)}$$
. (70)

As alluded to above, these two simplifications formally make the PFC theory different from CDFT, turning it instead into a type of Ginzburg-Landau type of field theory, where n represents an order parameter that becomes periodic in the solid state. As has been shown in the PFC literature, this apparently gross over-simplification of CDFT manages to correctly reproduce many of the qualitative physics of solidification, such as nucleation, grain boundary misorientation energy, elastic response and dislocations in the solid phase, vacancy diffusion and creep, grain boundary pre-melting, vacancy trapping, and numerous other effects. By progressively improving the parametrization of PFC theories, guided by

inspection of the underlying forms, PFC will be able to better quantitatively model the aforementioned processes.

X. SIMPLIFIED BINARY PHASE FIELD CRYSTAL MODELS

In this chapter, we review two simplified binary PFC models: the original binary PFC model of Elder et al. [18] and the binary structural PFC (XPFC) model of Greenwood et al. [19]. We begin by outlining the binary PFC background, followed by a summary and comparison of each model.

XI. BINARY PFC BACKGROUND

The multicomponent free energy functional for binary PFC

$$g[\rho_{A}, \rho_{B}] = \frac{g(r) \ln \frac{\rho_{i}(r)}{\rho_{i}^{0}}}{\frac{1}{\rho_{i}^{0}}} - (1 - \beta \mu^{0}) \Delta \rho_{i}(r)$$

$$\frac{1}{2} \sum_{i=A} \Delta \rho_{i}(r) * G^{(2)}_{i}(r, r') * \Delta \rho_{i}(r').$$

$$\frac{1}{2} \sum_{i=A} \Delta \rho_{i}(r) * G^{(2)}_{i}(r, r') * \Delta \rho_{i}(r').$$

Using dimensionless density variables, the free energy functional can be rewritten as:

$$\frac{\beta F[n, c]}{\rho_0} = \frac{\beta F_{in}[n]}{\rho_0} + \frac{\beta F_{onin}[n, c]}{\rho_0} + \frac{\beta F_{onin}[n, c]}{\rho_0}. \quad (72)$$

The n-c correlations in the excess free energy are:

$$C_{AB} = \rho_0 c^2 C_{BB} + (1 - c)^2 C_{AA} + 2c(1 - c) C_{AB}$$
, (73)

$$C_{AB} = \rho_0 \left(cC_{BB} - (1 - c)C_{AB} + (1 - 2c)C_{AB} \right),$$
 (74)

$$C_{AA} = \rho_0 (C_{BB} + C_{AA} - 2C_{AB})$$
....(76)

XII. ORIGINAL BINARY PFC MODEL

The original binary PFC model expands the free energy around n(r) = 0 and $c(r) = c_0$:

$$\frac{\partial F_{ij}[n]}{\partial r} = \int \frac{\alpha(r)^2}{r^2} - \eta \frac{\alpha(r)^3}{r^2} + * \frac{\alpha(r)^4}{r^2} . \quad (77)$$

The excess free energy is simplified using a gradient expansion:

$$C_{rr}(r, r') = C_0 + C_2 \nabla^2 + C_4 \nabla^4 \delta(r - r'),$$
 (78)

$$C_{\omega}(r, \dot{r}) \equiv -\varepsilon + W_{\omega}\nabla^2 \delta(r - \dot{r}).$$
 (79)

This model, though capable of simulating eutectic and dendritic growth, is limited to forming only BCC phases due to its simplified correlation function.

XIII. BINARY STRUCTURAL PHASE FIELD CRYSTAL MODEL

The XPFC model improves the original by retaining the full free energy of mixing and enhancing the control over the density-density correlation function:

$$\tilde{\zeta}(k) = \frac{1}{\alpha} e^{\frac{T}{T_0}} e^{-\frac{(k-k_0)^2}{2\sigma_0^2}}.$$
(80)

This formulation allows the XPFC model to describe a variety of crystal lattice structures and phase diagrams over a wide range of concentrations.

XIV. IMPROVEMENTS TO THE BINARY XPFC MODEL

In this chapter, we present two significant enhancements to the binary XPFC theory. These improvements are novel contributions to the field, substantially extending the scope of the XPFC framework. The first enhancement involves modifying the free energy of mixing in the XPFC model by incorporating an enthalpy of mixing. The second improvement generalizes the phenomenological form of the two-point correlation function in binary alloys.

XV. ADDING AN ENTHALPY OF MIXING

the extension of the free energy of mixing beyond ideal mixing is achieved by removing the assumption made by Greenwood et al. that the concentration-concentration correlation function has no k = 0 mode. This approach is consistent with the original PFC model, while retaining the unexpanded, ideal mixing term as in the original XPFC alloy model. Specifically, the correlation function is expanded as:

$$C_{\infty}(r, r') = \delta(r - r') + \omega_{\epsilon} + \omega_{\epsilon} \nabla^{2} + \cdots$$
 (81)

The resulting model has a free energy of mixing equivalent to the regular solution model, establishing a clear connection with widely-used models in materials science. This formulation captures the essential physics of a non-negligible enthalpy of mixing.

XVI GENERALIZING THE TWO-POINT CORRELATION FUNCTION

To develop a general phenomenology for modeling densitydensity correlation functions in alloys, we express the densitydensity correlation function as a linear combination of interpolating functions in concentration, $\zeta(c)$, multiplied by bare correlation functions C(r, r') of individual components:

$$C_{cos}(r, r'; c) = \frac{2}{\epsilon} \zeta(c) \zeta(r, r'),$$
 (82)

where the index i serves as an arbitrary label. In the original $C_{\text{cov}}(r,r') = C_0 + C_2 \nabla^2 + C_4 \nabla^4 \delta(r-r')$, (78) alloy CDFT theory (equation 22), for instance, we use the labels {AA, AB, BB} with interpolation functions:

$$\zeta_{0A}(c) = \rho_0(1 - c^2),$$
 (83)

$$\zeta_{AB}(c) = \rho_{0}c(1-c),$$
 (84)

$$\zeta_{BB}(c) = \rho_0 c^2$$
. (85)

This suggests a new definition to generalize the densitydensity correlation function for a binary alloy: The labels / enumerate the set of crystal structures present in the alloy system. The correlation functions, $\zeta_i(r, r')$, model the crystal structure I, and the associated interpolation functions $\zeta(c)$ define the concentration ranges where these correlations are valid.

A. Example: Silver-Copper Eutectic Alloy

For the silver-copper eutectic alloy system, we start with correlation functions for pure silver, $C_{\alpha}(r, r')$, and pure copper, $C_{\theta}(r, r')$. These two structures, the silver-rich α phase and the copper-rich β phase, are the only two relevant crystalline phases. To build the full density-density correlation function, we define interpolating functions for each phase:

$$\zeta_0(c) = 1 - 3c^2 + 2c^3$$
, (86)

$$\zeta_{\mathcal{S}}(c) = 1 - 3(1 - c)^2 + 2(1 - c)^3.$$
 (87)

Using the original XPFC formalism for bare correlation functions (equation 22), we can model the α and θ phases, which are both FCC [20], as in [21].

XVII EQUILIBRIUM PROPERTIES OF BINARY ALLOYS

These two modifications to the XPFC formalism allow us to study a broader range of systems. This section explores the equilibrium properties of the improved XPFC free energy functional, specialized for three different material phase disgrams: eutectic, syntectic, and monotectic.

A. Eutectic Phase Diagram

Previous PFC models have demonstrated that elastic energy is a sufficient driving force for eutectic solidification. Our regular solution XPFC model, however, enables an analysis of the role of enthalpy of mixing in eutectic solids. For instance, Murdoch and Schuh observed that in nanocrystalline binary alloys, while a positive enthalpy of segregation can stabilize against grain growth via solute segregation at the grain boundary, an excessively high enthalpy of mixing may lead to second phase formation or even macroscopic phase separation [22].

The pair correlation function used in the binary XPFC of Greenwood et al. can be recovered with the following choice of interpolation functions:

$$\zeta_{a}(c) = 2c^{8} - 3c^{2} + 1,$$
 (88)

$$\zeta_{\beta}(c) = \zeta_{\alpha}(1-c).$$
 (89)

Figure 2 shows the eutectic phase diagram for a triangular g and θ solid phase.

B. Syntectic, Phase Diagram

Our improved XPFC model can also study various invariant binary reactions that have not yet been examined using phase field crystal models, such as the syntectic reaction, $l_1+l_2 \rightarrow \alpha$. By setting the spinodal temperature \mathcal{I}_{ω} sufficiently high and using an appropriate concentration window function $\zeta(c)$, we can simulate a syntectic phase diagram (Fig. ??).

C. Monotectic Phase Diagram

The monotectic reaction, $l_1 - \alpha + l_2$, involves the decomposition of a liquid into a solute-poor solid and a solute-rich liquid. To model a monotectic, we set the spinodal temperature

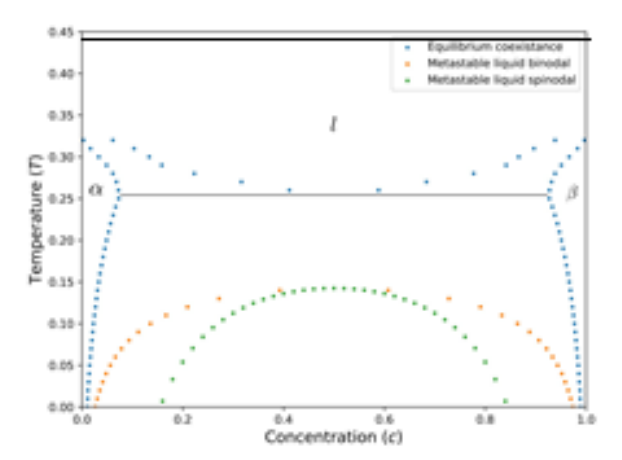


Fig. 2: Eutectic phase diagram for α and θ phases. Parameters: $\eta = 2, \chi = 1, \omega = 0.02, \epsilon_0 = 26.6$, and L = 0.15. Structure function parameters: $\sigma_{10\alpha} = \sigma_{10\beta} = 0.8$, $k_{10\alpha} = 2\pi$, $k_{10\beta} = 4\pi/3$, and $r_0 = 1$. The horizontal line denotes the eutectic temperature.

higher than the solidification temperature and use a window function centered at c = 0.

XVIII APPLICATIONS

This chapter explores applications of the enhanced binary XPFC model from Chapter XIV in microstructure evolution. We introduce phenom enological equations of motion for solute and density diffusion within the binary XPFC framework and apply them to study diffusion-limited precipitation from solution. Recent experiments on gold and silver nanoparticle precipitation [23] and calcium carbonate precipitation [24] have shown deviations from Classical Nucleation Theory (CNT), notably apinodal decomposition preceding nucleation in solute-rich phases. Here, we present preliminary findings supporting this dynamic behavior and demonstrate more complex post-nucleation growth beyond typical diffusive growth and coarsening. Future applications in precipitation studies and other areas are also discussed.

A. XPFC Dynamics

Following [19], we employ conservative dynamics for both n(x, t) and c(x, t):

$$\frac{\partial n(x, t)}{\partial t} = \Delta d_{xx} \nabla^{2} \frac{\delta(\beta \Delta F/\rho_{0})}{\delta n(x, t)} + \xi_{u}(x, t), \quad (90)$$

$$\frac{\partial c(x, t)}{\partial t} = M_{x} \nabla^{2} \frac{\delta(\beta \Delta F/\rho_{0})}{\delta c(x, t)} + \xi_{c}(x, t), \quad (91)$$

$$\frac{\partial c(x, t)}{\partial t} = M_c \nabla^2 \frac{\delta(\theta \Delta F/\rho_0)}{\delta c(x, t)} + \xi_c(x, t), \quad (91)$$

where M_{∞} and M_{∞} are mobilities, and $\xi_{\omega}(x, t)$ and $\xi(x, t)$ represent thermal fluctuations obeying the fluctuationdissipation theorem (see Appendix A). These equations are phenomenological, assuming local concentration conservation,

which holds when total density deviations are minimal ($c \approx g_{\omega}/\rho_0$).

XIX. MULTI-STEP NUCLEATION OF NANOPARTICLES IN SOLUTION

A. Nucleation Theories

Classical Nucleation Theory (CNT) describes the nucleation rate J via an Arrhenius expression:

$$J = A e^{-B \triangle G^{\dagger}}$$
 (92)

where A is a prefactor, ΔG^{\dagger} is the Gibbs free energy barrier, and n^{*} is the number of critical nuclei. The nucleation probability for a droplet of volume V is:

$$f_{evo}(t) = 1 - e^{-JV t}$$
. (93)

CNT assumes a single critical state characterized by a critical radius R*, often underestimating nucleation times due to oversimplified kinetic pathways [25], [26], [27]. Expanding the parameter space to include additional variables like density can improve agreement with experiments [25], but selecting appropriate parameters remains challenging.

Non-classical approaches, such as the XPFC alloy model, offer an unbiased framework to investigate nucleation without predefined parameters. By numerically integrating the equations of motion, the XPFC model can capture the full kinetic pathway on diffusive time scales, unlike molecular dynamics or traditional density functional theory.

B. Modeling Precipitation

To model systems like gold nanoparticle precipitation [23], we design a free energy functional with a submerged metastable spinodal beneath the liquid-solid coexistence curve [28]. This setup ensures that spinodal decomposition of the metastable liquid precedes nucleation from solution.

We center the interpolation function $\zeta_c(c)$ at c = 1 to favor the nanocrystalline solid α at high concentrations. The densitydensity correlation function for a 2D hexagonal precipitate is:

$$\tilde{C}_{QM}(k;c) = \exp \left(\frac{-(c-1)^2}{2\sigma_c^2} \right) = \exp \left(\frac{I}{\tau_0} \right) = \exp \left(\frac{-(k-k_{10})^2}{2\sigma_c^2} \right)$$

where g_s controls solvent solubility and k_{10} is the [10] reciprocal lattice vector length. An example phase diagram is shown in Figure 3, illustrating the metastable bipodal and spinodal below the coexistence curve.

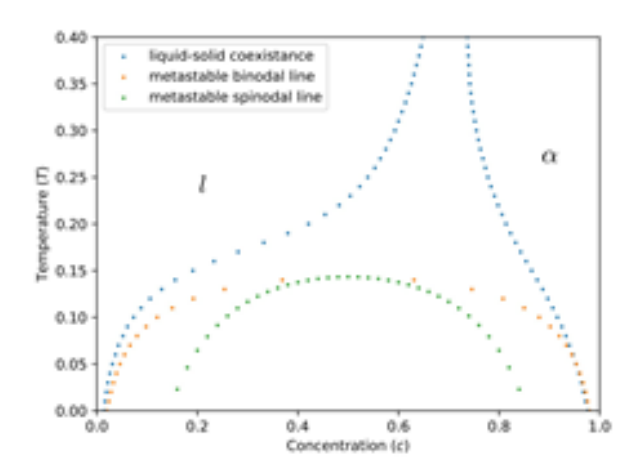


Fig. 3: Phase diagram of a precipitating solution with a hexagonal α solid phase. Parameters: 0.2, $\chi = 1$, $\omega = 0.3$, $\epsilon_0 = 30$, $\epsilon_0 = 0.15$, $\epsilon_0 = 0.5$. Correlation function parameters: $\sigma = 0.8$, $k_{10} = 2\pi$, $\tau_0 = 1$, $\sigma_0 = 0.5$.

C. Dynamics of Precipitation: Results and Discussion

We simulated precipitation by quenching a uniform solution (c = 0.3, n = 0.05) below the metastable apinodal ($T/T_0 = 0.07$). Figure 4 illustrates the microstructure evolution:

- Frames (a)-(c): Spinodal decomposition into solute-rich and poor regions.
- Frames (d)-(f): Nucleation of the solid phase within solute-rich regions.
- Frames (g)-(i): Growth and coarsening of nucleated nanoparticles.

This sequence consistently showed that once some soluterich regions crystallize, their growth accelerates, depleting solute from remaining regions—a phenomenon term ed sacrificial growth.

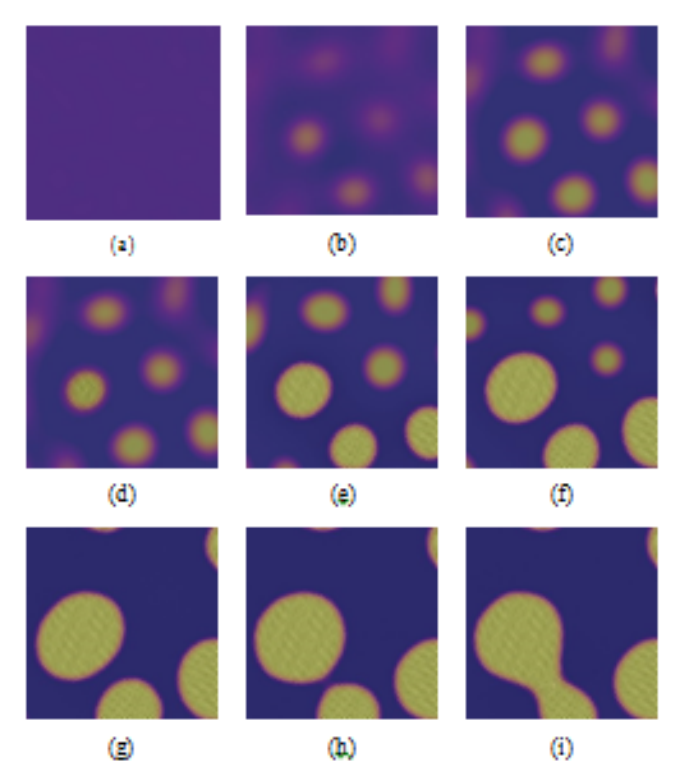


Fig. 4: Stages of nanoparticle precipitation: (a)-(c) Spinodal decomposition; (d)-(f) Nucleation and sacrificial growth; (g)-(i) Growth and coarsening. Parameters: c = 0.3, n = 0.05, $M_{\odot} = M_{\odot} = 1$, $M_{\odot} = 3.0$, $\Delta x = 0.125$, lattice size 1024 × 1024, $\Delta t = 0.0025$, T = 0.07.

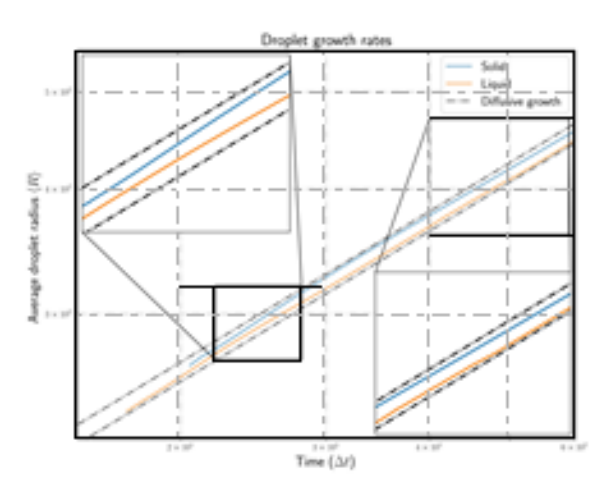


Fig. 5: Mean droplet radius $(\beta(t))$ yersus time on a log-log plot. The black line represents $\beta(t) \sim t^{1/2}$. Early stages exhibit hyper-diffusive growth, followed by hypo-diffusive coarsening.

Additionally, the fraction of uncrystallized droplets decreases significantly around 50% crystallization, as shown in Figure 6, indicating suppressed nucleation rates due to sacrificial growth.

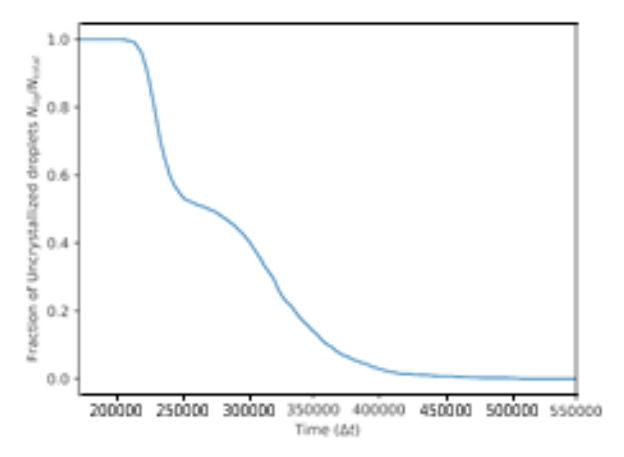


Fig. 6: Time evolution of the fraction of uncryatallized droplets. A sharp decline around 50% cryatallization reflects reduced nucleation rates.

XX. CONCLUSIONS AND FUTURE DIRECTIONS

This chapter demonstrates the application of the enhanced binary XPFC model to nanoparticle precipitation, supporting experimental observations of non-classical nucleation pathways involving apinodal decomposition preceding nucleation. The model reveals sacrificial growth dynamics, leading to a bimodal nanoparticle size distribution, aligning with experimental findings [23], [24]. Future work will refine the XPFC

To quantify this behavior, we analyzed the mean radius $\beta(t) = \frac{1}{2} (t)$ over 120 simulations. Purely diffusive growth predicts $(\beta(t)) \sim t^{1/2}$, while coarsening follows $(\beta(t)) \sim t^{1/3}$. Figure 5 displays $(\beta(t))$ on a log-log scale, revealing hyper-diffusive early growth transitioning to hypodiffusive coarsening.

model to incorporate factors like surface energy anisotropy and solvent effects, and extend applications to multi-component alloys, grain boundary dynamics, and phase transformations under external influences such as thermal gradients and fields. The versatility of the XPFC framework promises broad utility in advancing the understanding of complex material behaviors and designing materials with tailored properties.

XXI OUTLOOK AND FUTURE APPLICATIONS

The results presented describe the behavior of a quench followed by a multi-step precipitation process, relevant to the precipitation of gold nanoparticles observed in recent experiments. These predictions were made using a single framework based on the improved XPFC alloy model developed in this thesis. The dynamical results indicate a rich landscape of kinetic pathways for precipitation. Future applications include exploring the influence of quench parameters and solution concentration on nucleation kinetics and polydispersity of precipitated particles, key features of experimental interest.

XXII CONCLUSION

This research had three main goals: (1) introducing an enthalpy of mixing to account for non-ideal mixing (2) developing a phenomenology for modeling density pair correlation functions, and (3) applying these improvements to study multi-step nucleation pathways in precipitation. Chapter XIV detailed these extensions and their resulting equilibrium phase diagrams, capturing features like a submerged metastable liquid spinodal below the eutectic point Chapter XVIII showed that this model can reproduce multi-step nucleation pathways seen experimentally in silver and gold nanoparticles [23].

These improvements to the XPFC alloy model have further potential applications, such as studying elasticity effects on monotectic and syntectic nucleation and growth, as well as the stability of nanocrystalline binary alloys, which depend on the system's enthalpy of mixing [22].

APPENDIX

When using Langevin equations to study non-equilibrium statistical mechanics, the noise strength can be linked to the transport coefficients through a generalization of the Einstein relation. The generalization was first developed by Onsager and Machlup [29]. The typical strategy for deriving such a relationship is to evaluate the equilibrium pair correlation function by two separate methods: the equilibrium partition functional and the equation of motion8.

While the equilibrium partition functional gives pair correlation through the typical statistical mechanical calculation, the equation of motion can be used to derive a dynamic pair correlation function that must be equal to the equilibrium pair correlation function in the long time limit.

In what follows we'll look at how to formulate a generalized Einstein relation from a generic Langevin equation and then calculate two specific examples using Model A dynamics with

For considerations far from equilibrium see [30], [31], [32]

g ϕ^4 theory and Time Dependent Density Functional Theory (TDDFT) with a general Helmholtz free energy.

We start by considering a set of microscopic observables, g(f, t), that are governed by a nonlinear Langevin equation,

$$\frac{\partial \mathbf{a}(r, t)}{\partial t} = F |\mathbf{a}(r, t)| + \xi(r, t). \tag{95}$$

Where, a, denotes a vector of our fields of interest. These microscopic equation of motion may have been derived from linear response, projection operators or some other nonequilibrium formalism. We assume that the random driving force, $\xi(r, t)$ is unbiased, Gaussian noise that is uncorrelated

$$(\xi(r, t)) = 0, \qquad (96)$$

$$E \to \mathbf{L}(r, r')\delta(t - t'). \qquad (97)$$

$$\mathcal{E}(r, t) \xi^{\dagger}(r', t') = \mathbf{L}(r, r') \delta(t - t'). \quad (97)$$

This assumption is justified by positing that the stochastic driving force is the aggregated affect of many random microscopic processes that satisfy the central limit theorem so we may assume a Gaussian form. We wish to constrain the form of the covariance matrix, L, by demanding that the solution to the Langevin equation eventually decays to equilibrium and that correlations in equilibrium are given by Boltzmann statistics.

We begin by linearizing the equation of motion about an equilibrium solution, $\mathbf{a}(r, t) = \mathbf{a}_{nn}(r) + \hat{\mathbf{a}}(r, t)$.

$$\frac{\partial \hat{\mathbf{a}}(r, t)}{\partial t} - \mathbf{M}(r, r')_* \hat{\mathbf{a}}(r', t) + \xi(r, t) \qquad (98)$$

Where, *denotes an inner product and integration over the repeated variable, eg:

red variable.
$$\frac{\partial g}{\partial r}$$
:
 $\mathbf{M}(r, r') + \hat{\mathbf{a}}(r') = \frac{\sum_{i}^{j} dr' \mathcal{M}_{i}(r, r') \hat{\mathbf{a}}_{i}(r')}{dr' \mathcal{M}_{i}(r, r') \hat{\mathbf{a}}_{i}(r')}$. (99)

We can formally solve our linearized equation of motion,

$$\hat{\mathbf{a}}(r, t) = e^{\mathbf{M}(r, t)t} * \hat{\mathbf{a}}(r', 0) + \int_{0}^{\infty} d\mathbf{r} e^{\mathbf{M}(r, t)(t-r)} * \xi(r', \tau),$$
(100)

Considering the product $M(r, r_1)*\Gamma(r_1, r')$ and performing an integration by parts yields the final generalized Einstein

$$\mathbf{L}(r,r') = -\mathbf{M}(r,r_1) * \mathbf{\Gamma}(r_1,r'_1) + \mathbf{\Gamma}(r_1,r_1) * \mathbf{M}^{\dagger}(r_1,r'_1)$$
(101)

As we can see from equation 101, near equilibrium the noise correlation function is a simple function of the pair correlation function, $\Gamma(r, r')$ and the linearized transport coefficient $\mathbf{M}(r, r')$.

As a simple check we apply our result to the original work of Einstein. Recall that in the over damped limit the equation of motion for the velocity for a 1 dimensional Brownian particle is,

$$\frac{\partial v(t)}{\partial t} = -\frac{v(t)}{v(t)} + \xi(t).$$
 (102)

This equation is alread linear so we can pick off the linearized transport coefficient as -y. The pair correlation function in equilibrium is given by equipartition theorem as,

$$\frac{k_b T}{m}$$
. (103)

Simply applying equation 101 we find,

$$(\xi(t)\xi(t')) = 2 \int_{0}^{t} \frac{dt}{dt} \delta(t-t'),$$
 (104)

As expected. Satisfied that equation 101 reduces to the correct result for the base case we proceed to examine two examples that are guininely nonlinear field theories.

relation consider the following free energy functional under non-conservative, dissipative dynamics.

$$gF[\phi] = \int_{2}^{1} |\nabla \phi(x)|^{2} + \frac{r}{2} \phi^{2}(x) + \frac{u}{4!} \phi^{4}(x) + h(x)\phi(x)$$
(105)

$$\frac{\partial \phi(x, t)}{\partial t} = -\Gamma \frac{\delta \theta \Gamma[\phi]}{\delta \phi(x)} + \xi(x, t) \qquad (106)$$

The random driving force, ξ , is Gaussian noise, uncorrelated in time.

$$\langle \xi(x, t) \rangle = 0$$
 (107)

$$\langle \xi(x, t)\xi(x, t)\rangle = L(x - x)\delta(t - t)$$
 (108)

To compute the Einstein relation for this theory we start by calculating the pair correlation function using the equilibrium partition function and Boltzmann statistics.

A. The partition function route

In equilibrium the probability of particular field configuration is given by the Boltzmann distribution.

$$P_{ex}[\phi] = \frac{e^{-\theta F[\phi]}}{2!h(x)!}$$
(109)

Where, Z[h(x)] is the partition functional and is given by a path integral over all field configurations.

$$\sum [h(x)] = D[\phi]e^{-\theta F[\phi]} \qquad (110)$$

Evaluation of the partition function is of some importance because it plays the role of a moment generating function.

$$\frac{1}{Z[h]} \frac{\delta^{3}Z[h]}{\delta h(x_{1})...\delta h(x_{n})} = (\omega_{1}, \omega_{1}, \omega_{1}, \omega_{2}, \omega_{2}, \omega_{3}, \omega_{3})$$

$$(111)$$

In general the partition function cannot be computed directly, but in the special case of Gaussian free energies it can. To that end we consider expanding ϕ around an equilibrium solution, $\phi(x) = \phi_0 + \Delta \phi(x)$, and keeping terms to quadratic order in the free energy.

$$g_{F}[\Delta \phi] = dr \int_{-\infty}^{\infty} d\phi(x) r - \nabla^{2} + \int_{-\infty}^{\omega} d\phi(x) - h(x) \Delta \phi(x) Pair Correlation from the Partition Functional (112). The first term we can neglect as it adds an or$$

Here the partition function is written in a suggestive form. As stated previously, functional integrals are difficult to compute in general, but Gaussian functional integrals do have a

 Computing the Pair correlation function in the Gaussian approximation: To compute the pair correlation function we use the Fourier space variant of the partition function,

$$Z[\tilde{h}(k)] \propto \exp \frac{1}{2} \int_{\infty}^{\infty} \frac{h(k)h^*(k)}{r + \frac{\omega}{2}\phi^2 + |k|^2}$$
. (113)

The pair correlation function, $(\Delta \hat{\phi}(k) \Delta \hat{\phi}^*(k))$ is then computed using equation 111.

$${}^{D}_{\Delta \Phi(k) \Delta \Phi^{o}(k')} = \frac{2\pi \delta(k + k')}{r + \frac{\sigma}{2} \Phi_{0}^{2} + |k|^{2}}$$
(114)

The equation of motion supplies a second method for evaluating the pair correlation function in equilibrium.

$$\frac{\partial \phi}{\partial t} = -\Gamma \left(r - \nabla^2 \downarrow \phi(x, t) + \frac{u}{3!} \phi^3(x, t) + \xi(x, t), (115)\right)$$

Our equation of motion, can be linearized around an equilibrium solution, ϕ_0 just as we did in the partition function route to the pair correlation function. In a similar yain, we will Fourier transform the equation of motion as well.

$$\frac{\partial \Delta \tilde{\phi}(k, t)}{\partial t} = -\Gamma \left(r + \frac{U}{2} \phi + |k|^2\right) \Delta \tilde{\phi}(k, t) + \xi(x, t)$$
(116)

Comparing with our generalized approach we can read of M(k, k') from the lineared equation of motion:

$$M(k, k') = -\sum_{k} (r + \frac{u}{2} \phi_{0} + |k|^{2}) \delta(k + k')$$
 (117)

Finally, once we compute the generalized Einstein relation with our specific pair correlation and M(k, k') we find,

$$L(k, k') = 2\Gamma \delta(k + k'), \qquad (118)$$

Or equivalently,

$$L(x, x') = 2\Gamma\delta(x - x').$$
 (119)

In time dependent density functional theory (TDDFT) we have an equation of motion of the following form,

$$\frac{\partial P(r, t)}{\partial t} = D \nabla \cdot \rho(r, t) \nabla \cdot \frac{\partial V(p)}{\partial \rho} + \xi(r, t)$$
 (120)

Where, D_0 is the equilibrium diffusion constant and ξ is the stochastic driving force. We assume once again that the driving force has no bias, but we now allow the noise strength to be a generic kernel L(r, r').

$$\langle \xi(r, t) \rangle = 0$$
 (121)

$$\langle \xi(r, t)\xi(r', t') \rangle = L(r, r')\delta(t - t')$$
 (122)

The first term we can neglect as it adds an overall scale to the partition function that will not affect any of moments. Second moment only shifts the average so we can ignore it aş well and so we're left with a simple quadratic free energy once again.

$$F[\rho] = \frac{1}{2} \frac{dr}{dr} \frac{dr}{dr} \Delta \rho(r) \Gamma^{-1}(r, r) \Delta \rho(r) \qquad (123)$$

Where, $\Gamma^{-1}(r, r')$ is the second functional derivative of the free energy functional in equilibrium. Computing the pair correlation function from the partition function yields, as might be expected,

$$(\Delta \rho(r)\Delta \rho(r)) = \Gamma(r, r)$$
 (124)

D. Linearing the equation of motion

Linearizing the equation of motion about an equilibrium solution we find the following form.

$$\frac{\partial \Delta \rho(r, t)}{\partial r} = \frac{1}{2} \left(r\right) \nabla \Gamma^{-1}(r, r') * \Delta \rho (r', t) + \xi(r, t)$$
(125)

Once again we can read of the kernel M(r, r') from the linearized equation.

$$M(r, r') = D_0 \nabla \cdot \rho_{oo}(r) \nabla \Gamma^{-1}(r, r')$$
 (126)

Plugging into the generalized Einstein relation, we find a the factors of the pair correlation cancel giving a simple form for the kernel L(r, r').

$$L(r, r') = -2D_0\nabla \cdot (\rho_{ext}(r)\nabla) \delta(r - r')$$
 (127)

 Gaussian Functional Integrals: Solutions to this integral are not only important in there own right but are also the basis perturbative techniques. The detail of how to solve this integral can be found in [33] and are repeated here for the convenience of the reader.

This integral is simply the continuum limit of a multivariable Gaussian integral.

$$\mathbb{Z}[\mathbf{h}] = \begin{cases} dx_i \exp \left(\frac{1}{2} \sum_{i=1}^{\infty} \mathbf{x}_i \mathbf{K}_{ii} \mathbf{x}_i + \sum_{i=1}^{\infty} h \mathbf{K}_{ii} \right) \end{cases}$$
(128)

For which the solution is,

$$\mathbb{Z}[\mathbf{h}] = \frac{\mathbf{S}}{\det[\mathbf{K}]} \underbrace{\frac{2\pi}{2}}_{j} \underbrace{\frac{h}{h} \mathbf{K}^{-1}h}_{k = 0} . \quad (129)$$

In the continuum limit, the solution has an analogous form.

$$Z[b(x)] \propto \exp^{\int dx} \int dx' \frac{1}{2} h(x) \mathbf{K}^{-1}(x, x') h(x')$$
(130)

Where K^{-1} is defined by,

$$dx'K(x, x')K^{-1}(x', x'') = \delta(x - x'').$$
 (131)

Ultimately, we don't need to worry about the constant of proportionality in equation 130 because we'll be dividing this contribution when calculating correlation functions.

When developing the binary PFC model we often change variables from g_A and g_B to n and c. This change of variable is helpful in identifying the results of the PFC theory with

established results in the field as concentration and total density are more commonly used in the field of material science. Computing the bulk terms (i.e., $\Delta E_{col}[n, c]$ and $\Delta F_{col}[n]$ from equation ?? and ?? is a matter of substitution and simplification but computing the change of variables for excess free energy can be more subtle. When computing the pair correlation terms, careful application of our assumption that c varies over a much longer length scale than n must be applied to get the correct solution. The goal, ultimately, is to find C_{col} C_{col} C_{col} and C_{col} in the following expression,

(125)
$$\Delta \rho_A * \rho_0 C_{AA} * \Delta \rho_A + 2 \Delta \rho_A * \rho_0 C_{AB} * \Delta \rho_B + \Delta \rho_B * \rho_0 C_{BB} * \Delta \rho_B$$

1 the (132)
= $n * C_{oo} * n + 2n * C_{oo} * \Delta c + \Delta c * C_{oo} * \Delta c$,

We begin by rewriting $\Delta \rho_{ab}$

$$\Delta Q_{00} = Q_{00} - \rho_{00}$$
 $= Q_{00} - \rho_{00} + \rho_{00} - \rho_{00}$
 $= \Delta Q_{00} + \rho_{00} \Delta C_{0}$

And likewise $\Delta \rho_{a}$

$$\Delta g_A = g(1-c) - \rho_0(1-c_0)$$

= $\Delta g(1-c) - \rho_0 \Delta c$.

With those forms established, we demonstrate the general process by computing one term in equation 132: $\Delta \rho_B * C_{BB} * \Delta \rho_B$ We begin by expanding $\Delta \rho_B$

$$\Delta g_B * C_{BB} * \Delta g_B = (\Delta g_C + \rho_0 \Delta c) * C_{BB} * (\Delta g_C + \rho_0 \Delta c)$$

$$= \Delta g_C * C_{BB} * (\Delta g_C)$$

$$+ \rho_0 \Delta c * C_{BB} * (\Delta g_C)$$

$$+ \rho_0 (\Delta g_C) * C_{BB} * \Delta c$$

$$\pm g_0^2 \Delta c * C_{BB} * \Delta c.$$

If we examine one term in this expansion in detail, we note that we can simplify by using the long wavelength approximation for the concentration field,

$$\Delta \rho_{\mathcal{L}} C_{BB} * \Delta \rho_{\mathcal{L}} = \Delta \rho(r) c(r) \int_{0}^{\infty} dr' C_{BB}(r - r') \Delta \rho(r') c(r')$$

$$\approx \Delta \rho(r) c^{2}(r) \int_{0}^{\infty} dr' C_{BB}(r - r') \Delta \rho(r').$$
(135)

This is because the concentration field can be considered ostensibly constant over the length scale in which $C_{BB}(r)$ varies. Recall that the pair correlation function typically decays to zero on the order of several particle radii. Using this Volume 12, Issue 3: July - September 2025

approximation we can rewrite equation 134 as,

$$\Delta Q_B C_{BB} * \Delta Q_B = \Delta \rho c^2 C_{BB} * \Delta \rho$$

 $+ \rho_0 \Delta c (c C_{BB}) * \Delta \rho c$ (136)
 $+ \rho_0 \Delta \rho (c C_{BB}) * \Delta c$
 $+ \rho_0^2 \Delta c C_{BB} * \Delta c$.

Repeating this procedure with the remaining three terms and then regrouping we can easily identify the required pair correlations. 9

$$C_{AB} = \rho_0 c^2 C_{BB} + (1-c)_{\sim}^2 C_{AA} + 2c(1-c) C_{AB}$$
(137)
$$C_{AB} = C_{CD} = \rho_0 (c C_{BB} - (1-c) C_{AA} + (1-2c) C_{AB})$$
(138)
$$C_{CB} = \rho_0 (C_{BB} + C_{AA} - 2C_{AB})$$
(139)

This Appendix presents a general approach to integrating nonlinear stochastic partial differential equations. An integration scheme for the binary XPFC equations of motion is presented as a particular application.

To start, we consider the general case of time stepping a system of non-linear first-order PDE's. Specifically, we are going to look at a set of stochastic non-linear PDE's,

$$\frac{\partial \phi(x, t)}{\partial t} = G \quad \psi(x, t) + \xi(x, t), \quad (140)$$

Where,

<u>₩</u>(x, t) is a vector of our fields of interest (ex: (n, c)) and we've used - to denote a vector.

G is some driving force for our fields and,

 $\xi(x, t)$ is the stochastic driving force with variances given by a generalized Einstein relationship.

To develop a semi-implicit method we start by splitting the functional G into linear and non-linear components,

$$\frac{\partial \psi(x,t)}{\partial t} = \frac{1}{L} (x,x') \int_{-\infty} dt (x',t) + \int_{NL} \psi + \xi(x,t)$$
 (141)

Where,

- L denotes the linear contribution and "denotes a matrix,
- matrix multiplication and integration over the repeated variable and,

NL is the non-linear component of the the functional G.

In a special set of PDE's the kernel L is translationally invariant. When this is the case, the convolution theorem can be used to write the linear functional as an algebraic product in Fourier space.

$$\frac{\partial \overline{\psi}(k, t)}{\partial t} = \overline{\underline{L}}(k)\overline{\psi}(k, t) + F \text{ NJ}_{\omega}\overline{\psi} + \overline{\xi}(k, t)$$
 (142)

Where, H denotes a Fourier transform. We now consider our fields on a discrete grid with Δk spacing between Fourier modes and Δt spacing between times such that we might define.

$$\overline{\psi}_{i}^{"} \equiv \overline{\psi}(j\Delta k, n\Delta t).$$
 (143)

⁹Note that we may also take advantage of the fact that $C_{AB} = C_{BA}$.

To develop a generic approach to time stepping we consider evaluating our field between grid points in time (eg. at $\overline{\psi}_{\psi}^{n+\nu}$ where $\gamma \in [0, 1]$).

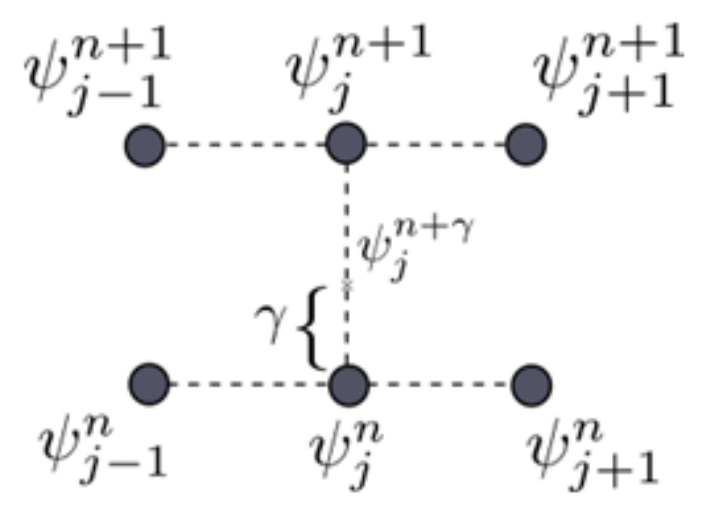


Fig. 7: Schematic of time step

To first order we can approximate this value as a linear interpolation of the value at n and the value at n + 1.

$$\overline{\psi_i} = (1 - \gamma)\overline{\psi_i} + \gamma \overline{\psi_i} \qquad (144)$$

We can also approximate the time derivative $\delta \psi$ as,

$$\frac{\partial \psi}{\partial t} = \frac{\psi_i^{\text{point}} - \psi_i^{\prime\prime}}{\Delta t} + \frac{1 - 2\nu}{4} \frac{\partial^2 \psi}{\partial t^2} \Delta t + ...$$
 (145)

Deriving different integration schemes is done by evaluating the equation of motion for various values of γ . For example, to recover simple Euler stepping we can evaluate the equation of motion with $\gamma = 0$. The semi-implicit scheme relays on evaluating the non-linear component of the equation of motion at $\gamma = 0$ while the rest of the equation is evaluated at $\gamma = 1$. In this treatment we will evaluate the non-linear component at $\gamma = 0$ but we will leave the rest of the equation unevaluated so that γ can be choosed freely at the end. Substituting these results into equation of motion we find the following result,

The final term on the right hand side emphasizes that if we choose y = 1/2 we will have a algorithm that is accurate to second order in time (this is a kind of Crank-Nicolson method). If we choose y = 1 we recover a semi-implicit method.

Important to note in the structure of \overline{L} is that it is diagonal in the limit of small ω . In the approximation that it is diagonal, previous algorithms for the binary XPFC model are recovered where, to linear order, concentration and density may be independently integrated. Another interesting case is that of $M_{\infty} = M_{\odot}$ where the matrix is symmetric and thus has orthogonal eigenvectors. We proceed by considering this simplified case where the concentration and density are weakly coupled at the linear order and may be integrated separately.

Volume 12, Issue 3: July - September 2025



E. Algorithm for the Concentration c(x, t)

The concentration equation of motion is,

$$\partial_{u}\zeta^{-} = -M_{c}k^{2} \ \omega_{c}\xi^{c} + W_{c}k^{2}\xi^{c} + \mathbb{E}\{NL(c)\} + \xi^{-}.$$
 (146)

Where NL(c) is the non-linear term and ξ is the drive noise.

$$NL(c) = \omega(1+n) \ln \frac{c}{c_0} - \ln \frac{1-c}{1-c_0} - \frac{1}{2}n C_{out}^n * n$$
(147)

Now if we think about the solution to this equation at time $t^{n+\xi}$ time between t^n and t^{n+1} we express the solution as an interpolation between the solutions at the earlier and later times.

$$-c_{k}^{-\alpha + \xi} = (1 - \xi)c_{k}^{-\alpha} + \xi c_{k}^{-\alpha + 1}$$
 (148)

We also find that we can express the time derivative as finite difference plus a correction term.

$$\alpha_{i}c = \frac{c^{n+1} - c^{n}}{\Delta t} + \frac{1 - 2\xi}{2} \frac{\partial^{2}c^{n}}{\partial t^{2}} \Delta t + ...$$
 (149)

Moving future times to the left and past times to the right we find,

$$c_k^{w+1} = \rho c_k^w + QF\{NL(c_k^w)\}_{k+L\xi_k} + \frac{2\xi - 1}{2} \frac{\partial^2 c_k^w}{\partial t^2} \Delta t$$
 (150)

Where the operators \hat{P} , \hat{Q} and \hat{L} are,

$$\hat{P} = 1 + \frac{\Delta t \Delta(k)}{1 - \xi \Delta t \Delta(k)}$$
(151)

$$Q = -\frac{M_c K^2 \Delta t}{1 - \Delta t \mathcal{E} \Lambda(k)}$$
(152)

$$Q = -\frac{M_c k^2 \Delta t}{1 - \Delta t \mathcal{E} \Delta(k)}$$

$$\hat{r} = \frac{\Delta t}{1 - \Delta t \mathcal{E} \Delta(k)}$$
(152)
$$\hat{r} = \frac{\Delta t}{1 - \Delta t \mathcal{E} \Delta(k)}$$

Different values of ξ lead to different integration schemes. The $\xi = 0$ corresponds to guler time stepping in fourier space, while $\xi = 1$ yields the often used semi-implicit fourier method. There is an import case in which we choose $\xi = 1/2$ where the algorithm becomes accurate to second order in time. This is the Crank-Nicholson fourier method.

F. Algorithm for the Total Density n(x, t)

We can develop an algorithm for the equation of motion to the total density in the same way that we did with concentration. The equation of motion for the total density in fourier space looks like,

$$\partial_{\nu} \tilde{U}(k, t) = -M_n k^2 (\tilde{n} + F\{NL(n)\}) + \tilde{\xi}$$
 (154)

Where now the nonlinear term is,

$$NL(n) = -\eta \frac{n^2}{2} + \chi \frac{n^8}{3} + \Delta f_{cris}(c) - C_{eff}^{\alpha} * n \quad (155)$$

Note that the convolution term is nonlinear because of an implicit dependance on the concentration. Now, in principle, you could compute that pair correlation function every time step for a more accurate linear propagator, but here we will not consider that.

Here again, we find the same structure as previously:

$$\tilde{H}_{L}^{n+1} = \hat{P} \stackrel{\text{d.c.}}{=} + \hat{Q} \stackrel{\text{E.(N L(al)}}{=} + \hat{L} \stackrel{\text{e. }}{=} k$$
 (156)

Here, the operators P, Q and L are:

$$\hat{\rho} = 1 - \frac{\Delta t M_n k^2}{1 + \xi \Delta t M_n k^2}$$
(157)

$$\hat{Q} = -\frac{M_c k^2 \Delta t}{1 + \Delta t \epsilon M_w k^2}$$
(158)

$$\hat{Q} = -\frac{M_c k^2 \Delta t}{1 + \Delta t \xi M_0 k^2}$$

$$\hat{I} = \frac{\Delta t}{1 + \Delta t \xi M_c k^2}$$
(158)

Volume 12, Issue 3: July - September 2025

ISSN 2394 - 7780

REFERENCES

- [1] E. T. Jaynes, "Information theory and statistical mechanics," Phys. Rev., vol. 106, pp. 620–630, May 1957. [Online]. Available: https://link.aps.org/doi/10.1103/PhysRev.106.620
- [2] E. Wigner, "On the quantum correction for thermodynamic equilibrium," Phys. Rev., vol. 40, pp. 749–759, Jun 1932. [Online]. Available: https://link.aps.org/doi/10.1103/PhysRev.40.749
- [3] J. G. Kirkwood, "Quantum statistics of almost classical assemblies," Phys. Rev., vol. 44, pp. 31–37, Jul 1933. [Online]. Available: https://link.aps.org/doi/10.1103/PhysRev.44.31
- [4] G. E. Uhlenbeck and E. Beth, "The quantum theory of the non-ideal gas ii. behavior of the virial coefficients," Physica, vol. 4, no. 8, pp. 729–745, 1937. [Online]. Available: https://www.sciencedirect.com/science/article/pii/S0031891438603462
- [5] L. Landau and E. Lifshitz, "Chapter ii: the gibbs distribution," in Statistical Physics (Third Edition, Revised and Enlarged), third edition, revised and enlarged ed., L. Landau and E. Lifshitz, Eds. Oxford: Butterworth-Heinemann, 1980, pp. 79–110. [Online]. Available: http://www.sciencedirect.com/science/article/pii/B9780750626360500071
- mup.//www.sciencedirect.com/science/article/ph/b//700/30020300300
- [6] W. Gibbs, Elementary principles in statistical mechanics, 1960.
- [7] R. Kubo, "Generalized cumulant expansion method," Journal of the Physical Society of Japan, vol. 17, no. 7, pp. 1100–1120, 1962. [Online]. Available: http://dx.doi.org/10.1143/JPSJ.17.1100
- [8] P. Espagnol and H. Löwen, "Derivation of dynamical density functional theory using the projection operator technique," The Journal of Chemical Physics, vol. 131, no. 24, p. 244101, 2009. [Online]. Available: http://dx.doi.org/10.1063/1.3266943
- [9] J.-P. Hansen and I. R. McDonald, "Appendix b: Two theorems in density functional theory," in Theory of Simple Liquids (Fourth Edition), fourth edition ed., J.-P. Hansen and I. R. McDonald, Eds. Oxford: Academic Press, 2013, pp. 587–589. [Online]. Available:

http://www.sciencedirect.com/science/article/pii/B9780123870322000272

- [10] J. E. Mayer and E. Montroll, "Molecular distribution," The Journal of Chemical Physics, vol. 9, no. 1, pp. 2–16, 1941. [Online]. Available: http://dx.doi.org/10.1063/1.1750822
- [11] J.-P. Hansen and I. R. McDonald, "Chapter 6 Inhomogeneous fluids," in Theory of Simple Liquids (Fourth Edition), fourth edition ed., J.-P. Hansen and I. R. McDonald, Eds. Oxford: Academic Press, 2013, pp. 203–264. [Online]. Available: http://www.sciencedirect.com/science/article/pii/B9780123870322000064
- [12] M. Oettel and S. A. Egorov, "Statistical mechanics of inhomogeneous fluids," Annual Review of Chemical Physics, vol. 9, no. 7, pp. 514–526, 1941. [Online]. Available: http://dx.doi.org/10.1063/1.1750822
- [13] M. Marconi and M. Yussouff, "First-principles order-parameter dynamics," Phys. Rev. B, vol. 19, pp. 2775–2794, Mar 1979. [Online]. Available: http://link.aps.org/doi/10.1103/PhysRevB.19.2775
- [14] T. Oxtoby, "The glass transition, the liquid-glass transition of the lennard-jones fluid," Advances in Chemical Physics, vol. 40, pp. 1–39, 1969. [Online]. Available: http://dx.doi.org/10.1002/9780470143594.ch1

- [15] J.-P. Hansen and L. Verlet, "Phase transitions of the lennard-jones system," Phys. Rev., vol. 184, pp. 151–161, Aug 1969. [Online]. Available: https://link.aps.org/doi/10.1103/PhysRev.184.151
- [16] U. M. B. Marconi and P. Tarazona, "Dynamic density functional theory of fluids," Journal of Physics: Condensed Matter, vol. 12, no. 8A, p. A413, 2000. [Online]. Available: http://stacks.iop.org/0953-8984/12/i= 8A/a=356
- [17] A. J. Archer and M. Rauscher, "Dynamical density functional theory for interacting brownian particles: stochastic or deterministic?" Journal of Physics A: Mathematical and General, vol. 37, no. 40, p. 9325, 2004. [Online]. Available: http://stacks.iop.org/0305-4470/37/i=40/a=001
- [18] K. R. Elder, N. Provatas, J. Berry, P. Stefanovic, and M. Grant, "Phase-field crystal modeling and classical density functional theory of freezing," Phys. Rev. B, vol. 75, p. 064107, Feb 2007. [Online].

Available: https://link.aps.org/doi/10.1103/PhysRevB.75.064107

- [19] M. Greenwood, N. Ofori-Opoku, J. Rottler, and N. Provatas, "Modeling structural transformations in binary alloys with phase field crystals," Phys. Rev. B, vol. 84, p. 064104, Aug 2011. [Online]. Available: https://link.aps.org/doi/10.1103/PhysRevB.84.064104
- [20] P. R. Subramanian and J. H. Perepezko, "The ag-cu (silver-copper) system," Journal of Phase Equilibria, vol. 14, pp. 62 75, 1993.
- [21] M. Greenwood, N. Provatas, and J. Rottler, "Free energy functionals for efficient phase field crystal modeling of structural phase transformations," Phys. Rev. Lett., vol. 105, p. 045702, Jul 2010. [Online]. Available: https://link.aps.org/doi/10.1103/PhysRevLett.105. 045702
- [22] H. A. Murdoch and C. A. Schuh, "Stability of binary nanocrystalline alloys against grain growth and phase separation," Acta Materialia, vol. 61, no. 6, pp. 2121 2132, 2013. [Online]. Available: http://www.sciencedirect.com/science/article/pii/S1359645412008919
- [23] N. D. Loh, S. Sen, M. Bosman, S. F. Tan, J. Zhong, C. A. Nijhuis,
- P. Kra'l, P. Matsudaira, and U. Mirsaidov, "Multistep nucleation of nanocrystals in aqueous solution," Nat Chem, vol. 9, Jan 2017.
- [24] A. F. Wallace, L. O. Hedges, A. Fernandez-Martinez, P. Raiteri, J. D. Gale, G. A. Waychunas, S. Whitelam, J. F. Banfield, and J. J. De Yoreo, "Microscopic evidence for liquid-liquid separation in supersaturated caco3 solutions," Science, vol. 341, no. 6148, pp. 885–889, 2013. [Online]. Available: http://science.sciencemag.org/content/341/6148/885
- [25] J. F. Lutsko and M. A. Duran-Olivencia, "A two-parameter extension of classical nucleation theory," Journal of Physics: Condensed Matter, vol. 27, no. 23, p. 235101, 2015. [Online]. Available: http://stacks.iop.org/0953-8984/27/i=23/a=235101
- [26] D. Knezic, J. Zaccaro, and A. S. Myerson, "Nucleation induction time in levitated droplets," The Journal of Physical Chemistry B, vol. 108, no. 30, pp. 10 672–10 677, 2004. [Online]. Available: http://dx.doi.org/10.1021/jp049586s
- [27] D. Erdemir, A. Y. Lee, and A. S. Myerson, "Nucleation of crystals from solution: Classical and two-step models," Accounts of Chemical Research, vol. 42, no. 5, pp. 621–629, 2009, pMID: 19402623.

[Online]. Available: http://dx.doi.org/10.1021/ar800217x

[28] R. J. Davey, S. L. M. Schroeder, and J. H. ter Horst, "Nucleation of organic crystals—a molecular perspective," Angewandte Chemie International Edition, vol. 52, no. 8, pp. 2166–2179, 2013. [Online].

Available: http://dx.doi.org/10.1002/anie.201204824

- [29] L. Onsager and S. Machlup, "Fluctuations and irreversible processes," Phys. Rev., vol. 91, pp. 1505–1512, Sep 1953. [Online]. Available: http://link.aps.org/doi/10.1103/PhysRev.91.1505
- [30] M. Lax, "Fluctuations from the nonequilibrium steady state," Rev. Mod. Phys., vol. 32, pp. 25–64, Jan 1960. [Online]. Available: http://link.aps.org/doi/10.1103/RevModPhys.32.25
- [31] D. Ronis, I. Procaccia, and J. Machta, "Statistical mechanics of stationary states. vi. hydrodynamic fluctuation theory far from equilibrium," Phys. Rev. A, vol. 22, pp. 714–724, Aug 1980. [Online].

Volume 12, Issue 3: July - September 2025

ISSN 2394 - 7780

Available: http://link.aps.org/doi/10.1103/PhysRevA.22.714

- [32] R. F. Fox and G. E. Uhlenbeck, "Contributions to non-equilibrium thermodynamics. i. theory of hydrodynamical fluctuations," Physics of Fluids, vol. 13, no. 8, pp. 1893–1902, 1970. [Online]. Available: http://scitation.aip.org/content/aip/journal/pof1/13/8/10.1063/1.1693183
- [33] M. Kardar, Statistical Physics of Fields, Jun. 2006.